

SUPPORTING INFORMATION

Rechargeable Sodium-ion Battery: High Capacity Ammonium Vanadate Cathode with Enhanced Stability at High Rate

Ananta Sarkar,¹ Sudeep Sarkar,¹ Tanmay Sarkar,² Parveen Kumar,² Mridula Dixit

Bharadwaj,² Sagar Mitra^{1}*

¹Electrochemical Energy Laboratory, Department of Energy Science and Engineering,

Indian Institute of Technology Bombay, Powai, Mumbai-400076, Maharashtra, India

²Center for Study of Science, Technology and Policy, 18, 10thCross, Mayura Street,

Papanna Layout, Nagashettyhalli, RMV II Stage, Bangalore-560094, Karnataka, India

Tel: + 91-222576-7849. E-mail: sagar.mitra@iitb.ac.in

First-principles calculations are based on Density Functional Theory (DFT) as implemented in Vienna Ab-initio Simulation Package (VASP).¹ We use a generalized gradient approximation (GGA) with the Perdew-Burke-Ernzerhof (PBE)² functional of the exchange and correlation energy. In the initial structure, the NH_4^+ ion lie between the layers and Na^+ ions, are present into the gallery space as well as within the layers.³ All the structures are fully relaxed through minimization of energy till the magnitude of forces is smaller than 0.02 eV \AA^{-1} and pressure less than 0.01 Kbar. We used an energy cut-off of 500 eV on the plane wave basis set and k-mesh grids of 3x9x9 for sampling Brillouin Zone integrations. We used $U = 3.0$ eV (Hubbard parameter) to incorporate onsite correlations of electrons in d orbitals of V in all the calculations. We calculated average electrochemical potential from Nernst equation

$$V_{cell} = \frac{-\Delta G}{nF} \approx \frac{-\Delta E}{nF} = -(E_{in-Na} - E_{de-Na} - E_{Na})$$

where V_{cell} is the cell voltage, ΔG is change in Gibbs free energy per mole which is approximate equal to change in calculated total energy ΔE , n is the number of moles of electrons transferred and F is the Faraday constant. E_{in-Na} , E_{de-Na} and E_{Na} are total energy are the energies per formula unit of sodiated and de-sodiated structures of electrode and one mol of Na atom, respectively (Figure S2).

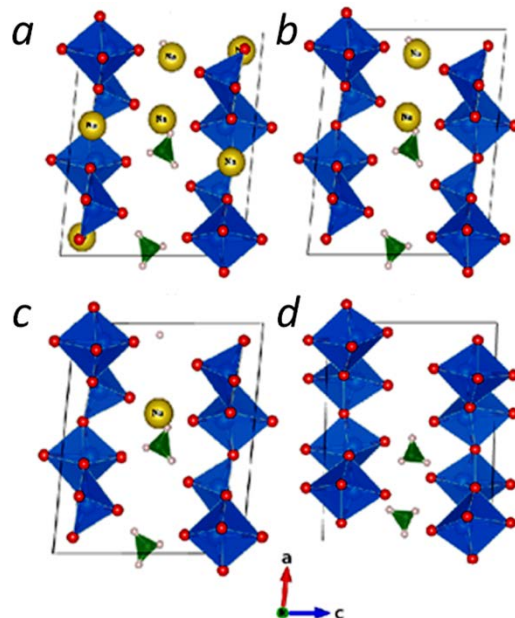


Figure S1. Configuration of the (a) $\text{Na}_3\text{NH}_4\text{V}_4\text{O}_{10}$. (b) $\text{Na}_1\text{NH}_4\text{V}_4\text{O}_{10}$. (c) $\text{Na}_{0.5}\text{NH}_4\text{V}_4\text{O}_{10}$. (d) $\text{NH}_4\text{V}_4\text{O}_{10}$.

Table S1. Magnetic moment of all the Vanadium atoms in $\text{Na}_x\text{NH}_4\text{V}_4\text{O}_{10}$ from DFT calculations.

| $\text{Na}_x\text{NH}_4\text{VO}_{10}$ | V1 | V2 | V3 | V4 | V5 | V6 | V7 | V8 |
|--|-----|-----|-----|-----|-----|-----|-----|-----|
| 0 | 0.2 | 0 | 1 | 0 | 0 | 0.2 | 0 | 1 |
| 0.5 | 0.2 | 0.2 | 0.7 | 0.3 | 0.2 | 1 | 1 | 0.2 |
| 1 | 1 | 0.2 | 0.3 | 1 | 0.2 | 1 | 1 | 0.3 |
| 3 | 1.1 | 1.1 | 1.1 | 1.1 | 1.1 | 1.1 | 1.1 | 1.1 |

Table S2. Calculated lattice parameters and lattice volume at different concentration of Na in $\text{NH}_4\text{V}_4\text{O}_{10}$.

| $\text{Na}_x\text{NH}_4\text{V}_4\text{O}_{10}$ 10 | Lattice parameter | | | Volume(\AA^3) |
|---|----------------------------|--------------------------|--------------------------|--------------------------|
| | a(\AA) | b(\AA) | c(\AA) | |
| 0 | 11.78(11.71 [#]) | 3.74(3.66 [#]) | 9.75(9.72 [#]) | 428.91 |
| 0.5 | 11.79 | 3.74 | 9.71 | 426.55 |
| 1 | 12.07 | 3.77 | 9.08 | 413.49 |
| 3 | 12.51 | 3.94 | 9.85 | 484.4 |

JCPDS File No. 31-0075.

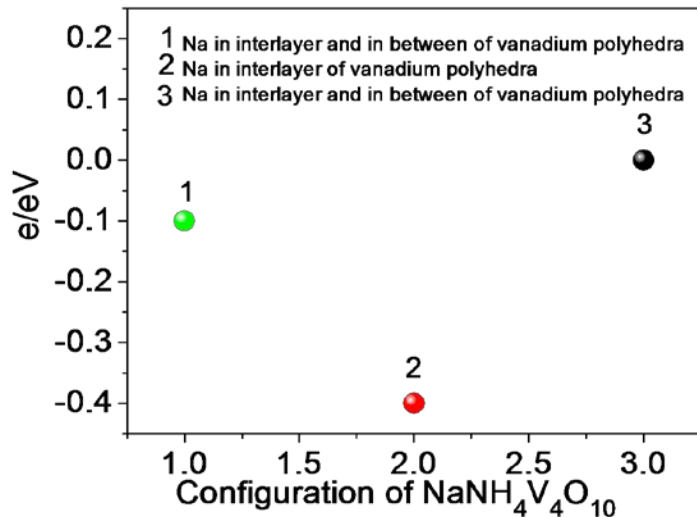


Figure S2. The calculated formation energies of $\text{NH}_4\text{V}_4\text{O}_{10}$ structure with Na in gallery space and within the layer.

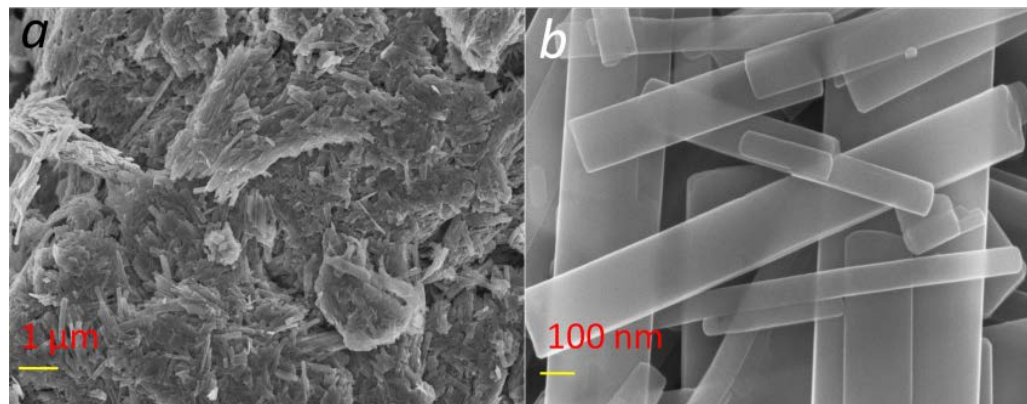


Figure S3. (a-b) FEG-SEM image of $\text{NH}_4\text{V}_4\text{O}_{10}$ nano-belts.

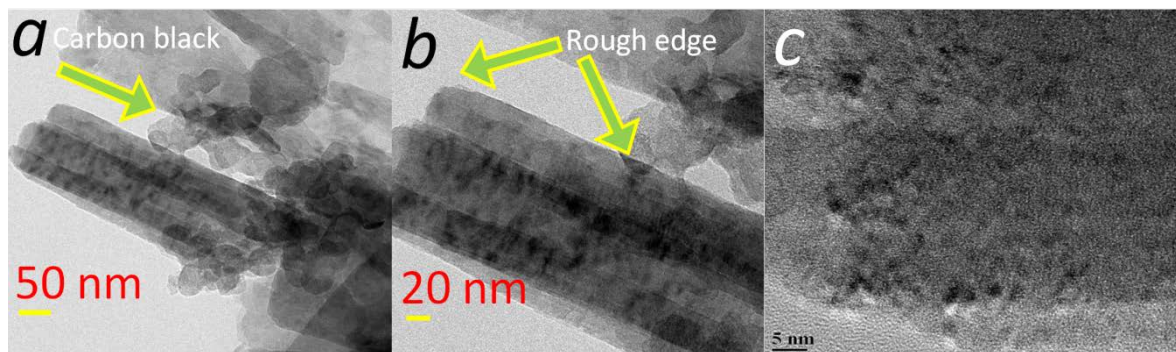


Figure S4. (a-b) FEG-TEM image. (c) HR-TEM image of $\text{NH}_4\text{V}_4\text{O}_{10}$ material (after 25thcycle).

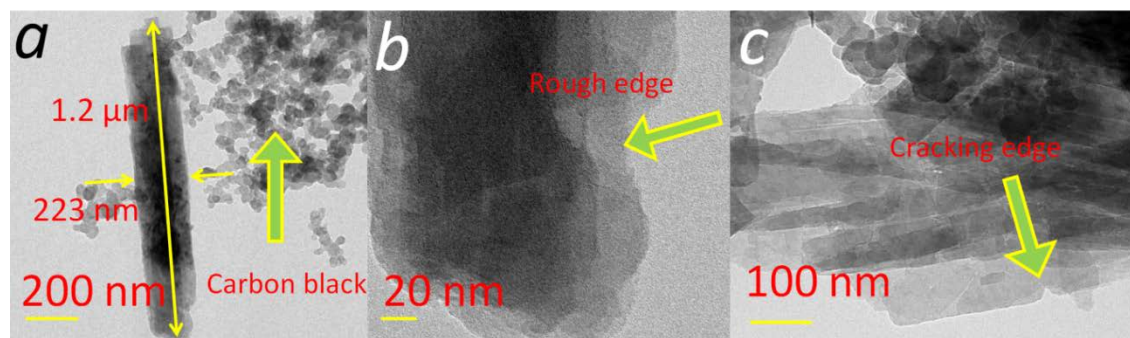


Figure S5. (a-c) FEG-TEM image of $\text{NH}_4\text{V}_4\text{O}_{10}$ material (after 32th cycle).

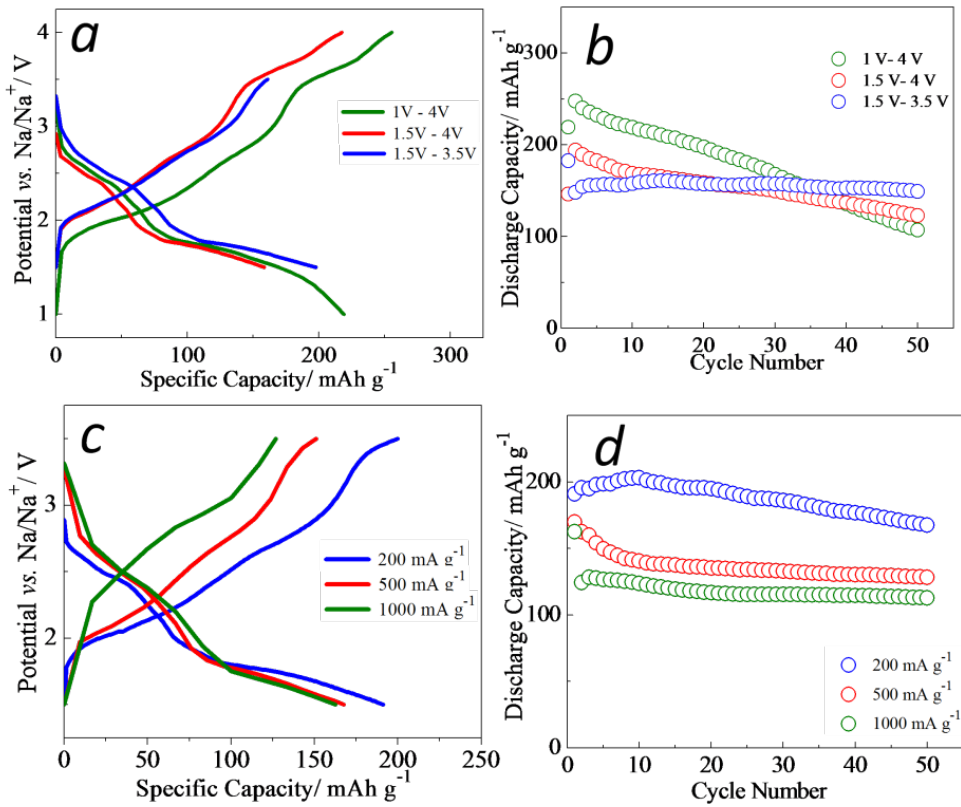


Figure S6. (a) 1st charge/discharge profile of $\text{NH}_4\text{V}_4\text{O}_{10}$ cathode material between varying potential (bare Al-current collector). (b) Discharge capacity vs. cycle number (bare Al-current collector), (c) 1st charge/discharge of $\text{NH}_4\text{V}_4\text{O}_{10}$ cathode material between 1.5-3.5 V at varying current rate with carbon coated Al-current collector. (d) Discharge capacity vs. cycle number between 1.5-3.5 V at varying current rate with carbon coated Al-current collector.

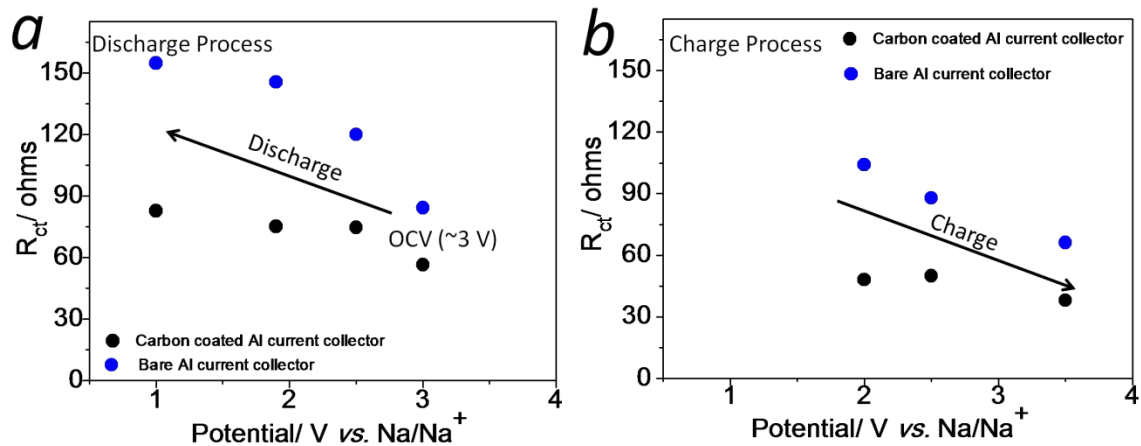


Figure S7. R_{ct} of Carbon coated and bare Al current collector during (a) Discharge process. (b) Charge process.

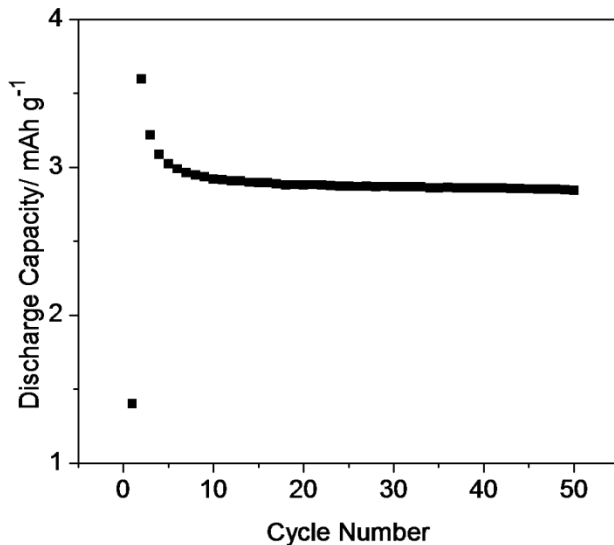


Figure S8. Discharge capacity of carbon at 200 mA g⁻¹ current rate between potential window 1.5 V-3.5 V.

The capacity contribution from conductive carbon is shown in Figure S8 which is ~ 3 mAh g⁻¹ at 200 mA g⁻¹ current rate (experiment done only with conductive carbon) between potential window of 1.5 V-3.5 V. Moreover, Na⁺ storage in conductive carbon was negligible compared to the NH₄V₄O₁₀ cathode material with and with-out carbon coated Al current collector.

REFERENCES

1. Kresse, G.; Furthmuller, J. Efficiency of Ab-initio Total Energy Calculations for Metals and Semiconductors Using a Plane-wave Basis Set. *Comput. Mater. Sci.* **1996**, *6*, 15-50.
2. Perdew, J.; Burke, K.; Ernzerhof, M. Generalized Gradient Approximation Made Simple. *Phys. Rev. Lett.* **1996**, *77*, 3865-3868.
3. Kim, H.; Kim, D. Y.; Kim, Y.; Lee, S.; Park, K. Na Insertion Mechanisms in Vanadium Oxide Nanotubes for Na-Ion Batteries. *ACS Appl. Mater. Interfaces* **2015**, *7*, 1477-1485.